Shock-induced $\alpha-\omega$ transition in titanium

C. W. Greeff,[a)] D. R. Trinkle, and R. C. Albers

Los Alamos National Laboratory, Los Alamos, New Mexico 87545

Equilibrium free energies for the α and ω phases of Ti are constructed. The result is a consistent picture of the ambient pressure, static high pressure, and shock data, as well as first-principles electronic structure calculations. The Hugoniot consists of three segments: a metastable α-phase region, a transition region, and an ω-phase branch. All the Hugoniot data are consistent with a transition occurring at ~12 GPa. An early identification [R. G. McQueen *et al.*, in *High Velocity Impact Phenomena*, edited by R. Kinslow (Academic, New York, 1970)] of a phase transition at 17.5 GPa appears to have been an artifact. The shock Hugoniot extends further into the metastable region than static data, indicating the existence of a relaxation process occurring on a time scale intermediate between those of the static and dynamic measurements. © *2001 American Institute of Physics.* [DOI: 10.1063/1.1389334]

I. INTRODUCTION

The pressure driven transition from the α (hcp) to the ω phase in Ti was first observed by Jameison,[1] and has since been studied extensively with static high pressure[2–7] and shockwave[8–11] techniques. The phase diagram of Ti, including the α, ω, and high-temperature β (bcc) phases was mapped by Bundy.[2] Room temperature studies on the $\alpha-\omega$ transition show large hysteresis, with the high-pressure omega phase being retained after pressure is released.[3] The onset of the transition has been observed over a wide range of pressures from 2.9[5] to 9.0[2] GPa. This variability may be due to in part to differences in sample purity, which has been observed to influence the transformation kinetics. Application of shear stress was found to reduce the hysteresis of the transformation, allowing the equilibrium transition pressure at room temperature to be estimated at 2.0 ± 0.3 GPa.[4] Shock Hugoniot measurements show anomalies in the curve $U_s(U_p)$ relating the shock and material velocities.[8,11] Time-resolved shock wave profiles show the characteristic structure associated with a phase transition.[9,10] High-purity samples were found to retain ω phase after having been shocked to 11 GPa,[10] indicating that the shock anomaly is associated with the $\alpha-\omega$ transition.

In the present work, we present results of our efforts to develop accurate equilibrium thermodynamic functions to describe the $\alpha-\omega$ transition in Ti. This work is fundamental for continuum level simulations of shock wave propagation in solids, which require accurate equations of state. For media undergoing phase transitions, at least a phenomenological description of phase transition kinetics is required for accurate calculations of wave profiles.[14,15] In attempting to go beyond phenomenology, accurate equilibrium quantities are needed as a basis for more physical models of nonequilibrium processes. For these reasons, we have developed free energy functions for the α and ω phases of Ti. The approach is to use functional forms for the free energy that are based

on solid state physics. The functions contain parameters that are empirically adjusted. The data used include ambient pressure thermodynamic data, static high-pressure measurements, the phase boundary, and shock Hugoniot. As an additional check, we have done first principles electronic structure calculations of the cold energies. The empirical cold energy curves are in very good agreement with the first principles calculations, apart from a small shift of the ω-phase relative to α, confirming our understanding of the data. The result is a consistent picture unifying the ambient, static high-pressure, and shock data, as well as fundamental theory.

II. METHODS

Our empirical Helmholtz free energy is based on the functional form[15]

$$F(V,T) = \phi_0(V) + F_{\text{vib}}(V,T) + F_{\text{el}}(V,T). \quad (1)$$

Here $\phi_0(V)$ is the static lattice potential, the energy with all atoms fixed at their ideal crystal positions. It is directly comparable with the band structure total energy. We use the universal isotherm of Rose *et al.*[16] for $\phi_0(V)$:

$$\phi_0(V) = \phi^* + \frac{4V^* B^*}{(B_1^* - 1)^2} [1 - (1 + \eta)e^{-\eta}]$$

$$\eta = \frac{3}{2}(B_1^* - 1)\left[\left(\frac{V}{V^*}\right)^{1/3} - 1\right]. \quad (2)$$

The parameters are the equilibrium volume, V^*, and B^* and B_1^*, the bulk modulus and its pressure derivative, respectively, at the equilibrium volume. The parameter ϕ^* controls the relative energy of the two phases. F_{vib} denotes the lattice vibrational free energy, which is taken to be quasiharmonic, and the high-temperature expansion is used[17]

$$F_{\text{vib}}(V,T) = 3kT\left(-\ln[T/\theta_0(V)] + \frac{1}{40}[\theta_2(V)/T]^2\right), \quad (3)$$

where θ_0 and θ_2 are moments of the phonon spectrum,

[a)]Electronic mail: greeff@lanl.gov

2221

$$\ln(k\theta_0) = \langle \ln(\hbar\omega) \rangle_{\text{BZ}}$$

$$(k\theta_2)^2 = \frac{5}{3} \langle (\hbar\omega)^2 \rangle_{\text{BZ}}, \tag{4}$$

and $\langle \rangle_{\text{BZ}}$ denotes an average over the Brillouin zone. Equation (3) is equivalent to the first two terms in the high-temperature expansion given by Wallace[17] as his Eq. (19.26). The notation used here is that of Boettger and Wallace.[15] The first term is the classical free energy of a harmonic lattice[18] and the second term is a quantum correction. Note that in our applications, the high-temperature series is rapidly convergent and the second term in Eq. (3) is small. The volume dependence of θ_0 is given through the Gruneisen parameter

$$\gamma = -d\ln(\theta_0)/d\ln(V), \tag{5}$$

with γ assumed to follow

$$\gamma(V) = \gamma_0 V/V_0, \tag{6}$$

and V_0 is a reference volume. In the notation of Anderson,[19] Eq. (6) corresponds to $q = d\ln\gamma/d\ln V = 1$. Over the range of densities considered here, we do not expect our results to be sensitive to this approximation. The second term in Eq. (3) is a small correction in our applications, so we use the approximation $\theta_2 = e^{1/3}\theta_0$ (e is the base of the natural logarithms) at all V.[12,20] The electronic excitation free energy, $F_{\text{el}}(V,T)$, is taken to have the low-temperature, Fermi liquid form

$$F_{\text{el}}(V,T) = -\frac{1}{2}\Gamma(V)T^2, \tag{7}$$

where $\Gamma(V)$ is proportional to the density of states at the Fermi surface. Its volume dependence is taken to be

$$\Gamma(V) = \Gamma_0(V/V_0)^\kappa. \tag{8}$$

We have used the following data sources in adjusting the model parameters: ambient pressure specific heat and entropy from Refs. 21 and 22; bulk modulus from Ref. 23; pressure dependence of the bulk modulus from Ref. 24; thermal expansion from Ref. 25; phonon spectrum from Ref. 26; equilibrium volume of α phase from Ref. 27; volume of ω phase from Refs. 1 and 3; high pressure room temperature isotherm from Refs. 6 and 7; shock Hugoniot from Refs. 8 and 11; calculated electronic densities of states from Refs. 12 and 13. There is some uncertainty as to the location of the equilibrium α–ω phase boundary, given the hysteresis and impurity effects. We have chosen to use the room temperature transition pressure of 2.0 GPa from Zilbershteyn et al.,[4] and the α–β–ω triple point at $T = 910$ K, $P = 9.4$ GPa, from Bundy[2] to fix the phase boundary. At the triple point temperature, hysteresis is small.[2]

We calculate Hugoniot states by solving the jump condition

$$E - E_0 = \frac{1}{2}(\sigma + \sigma_0)(V - V_0), \tag{9}$$

where σ is the normal stress. For the most part, we neglect strength and set $\sigma = -P$, where P is the thermodynamic

pressure, then Eq. (9) can be solved for T, given V. Final states may be in a two-phase coexistence region, in which case we have

$$E = (1-\lambda)E_1(V_1,T) + \lambda E_2(V_2,T)$$

$$V = (1-\lambda)V_1 + \lambda V_2, \tag{10}$$

together with the conditions of equilibrium

$$P_1(V_1,T) = P_2(V_2,T)$$

$$G_1(V_1,T) = G_2(V_2,T), \tag{11}$$

where G is the Gibbs free energy. Eqs. (9)–(11) allow one to solve for V_1, V_2, λ, and T given V. We refer to this solution as the equilibrium Hugoniot. Equality of the Gibbs free energies is usually relaxed in phenomenological treatments of nonequilibrium.

The strength of Ti is large, and has a nonnegligible impact on the Hugoniot, especially at low pressure. This has two effects on the Hugoniot calculation. First, the jump condition Eq. (9) refers to the P_1 wave, and its initial state is at the Hugoniot elastic limit (HEL), not ambient pressure. Second, the deviatoric part of the normal stress is not zero. We make the simplifying assumptions that the yield stress and shear modulus are constants. Then the deviatoric part of the normal stress is a constant at the HEL and above, and

$$(\sigma + \sigma_0) = -(P + P_{\text{HEL}} + 2\Delta P). \tag{12}$$

We estimate the deviatoric part of the normal stress ΔP using linear elasticity as (our ΔP is $4/3\tau$ in the notation of Ref. 28)

$$\Delta P = |\sigma_{\text{HEL}}| \bigg/ \left(\frac{3B}{4G} + 1\right), \tag{13}$$

where B and G are the bulk and shear modulus, respectively. Our procedure for strength corrections to the Hugoniot is then to estimate the parameters of the HEL state using linear elasticity and assuming that the compression to the HEL point is adiabatic. We then solve the jump condition, Eq. (9), for the P_1 wave with the HEL as initial point, while accounting for the deviatoric stress according to Eqs. (12) and (13). This procedure is not applicable when the plastic transition is overdriven, and we use it only at pressures for which there is an elastic precursor.

The total energy calculations for titanium in the hcp and omega structure were performed using the WIEN97[29] code. It is a full-potential LAPW code, and we used the generalized-gradient approximation as parameterized by Perdew, Burke, and Ernzerhof.[30] A muffin-tin radius of 2.0 atomic units was used, with an $R_{\text{MT}}K_{\text{max}}$ of 9.0. The k-point mesh for the hcp structure was an $18 \times 18 \times 12$ mesh, and a $12 \times 12 \times 18$ mesh was used for the omega structure calculations. The modified tetrahedron method of Bloechl[31] was used to calculate total energies. Finally, for each volume, the c/a ratio was relaxed to find the minimum energy for that volume.

III. RESULTS

The numerical values of our final free energy parameters are given in Table I. Some thermodynamic quantities from

TABLE I. Parameter values for free energies of α and ω Ti.

	α	ω	units
V_0	10.631	10.460	cm^3/mol
θ_{00}	252.0	263.4	K
γ_{00}	1.17	1.65	
Γ_0	4.6×10^{-3}	4.45×10^{-3}	J/(K^2 mol)
κ	1.45	1.40	
V^*	10.545	10.350	cm^3/mol
B^*	110.08	118.0	GPa
B_1^*	4.3	3.05	
ϕ_0^*	0.0	-60.0	J/mol

FIG. 1. Temperature dependence of the entropy of Ti at ambient pressure. Symbols are data from Refs. 21 and 22. Dotted curve is present free energy, dashed curve is vibrational component only.

our free energy are compared with experimental values in Table II. We note that there are enough parameters to exactly match c_P and S, however, to do so would require modifying θ_{00}, which is taken from neutron scattering data.[26] Thus, the chosen parameters represent a compromise between all the data. Also, we did not simply match the ambient temperature data but rather attempted to match the specific heat, entropy, and thermal expansion over a wide temperature range. This is illustrated in Fig. 1, which shows the entropy as a function of temperature at ambient pressure. There is not any combination of parameters that would allow us to match simultaneously the temperature[23] and pressure[24] dependence of the bulk modulus B_S. Once the thermal expansion is fixed $(\partial B_S / \partial T)_P$ is essentially determined by B_1^*, the same parameter that dominates $(\partial B_S / \partial P)_T$. Matching $(\partial B_S / \partial T)_P$ gives the value $B_1^* = 5.4$. The present value of 4.3 was chosen to match $(\partial B_S / \partial P)_T$, since this is more relevant to the shock process. Varying B_1^* over this range makes a small but noticeable difference in the slope of the α phase Hugoniot. We return to this sensitivity in our discussion of the Hugoniot below.

The α-phase free energy is over constrained by the data. The data for the ω phase are more limited, and the parameters are not as well constrained. We have used results from band structure calculations[13] to estimate Γ_{00}. The calculations of Eriksson et al.[12] were used to constrain the value of κ, which has a weak effect on the results. The value of θ_{00}, which is the dominant contributor to ΔS, the change in entropy at the transition, is adjusted to give the slope of the phase boundary. The remaining parameters are adjusted on the basis of the room temperature $P(V)$ data, and the high-pressure part of the Hugoniot.

Figure 2 shows the room temperature isotherm at high pressure along with the diffraction data.[6,7] These data

TABLE II. Thermodynamic properties of α Ti. β denotes the volumetric thermal expansion coefficient, $\beta = V^{-1}(\partial V/\partial T)_P$. Other symbols have standard meanings.

	Free energy	Expt	Units	Source (Ref.)
c_P	24.8	25.2	J/(mol K)	21, 22
S	31.4	30.7	J/(mol K)	21, 22
B_S	107.3	107.3	GPa	23, 24
$(\partial B_S/\partial T)_P$	-0.8	-1.2	10^{-2} GPa/K	23
$(\partial B_S/\partial P)_T$	4.33	4.31		24
β	2.58	2.58	10^{-5} K^{-1}	25
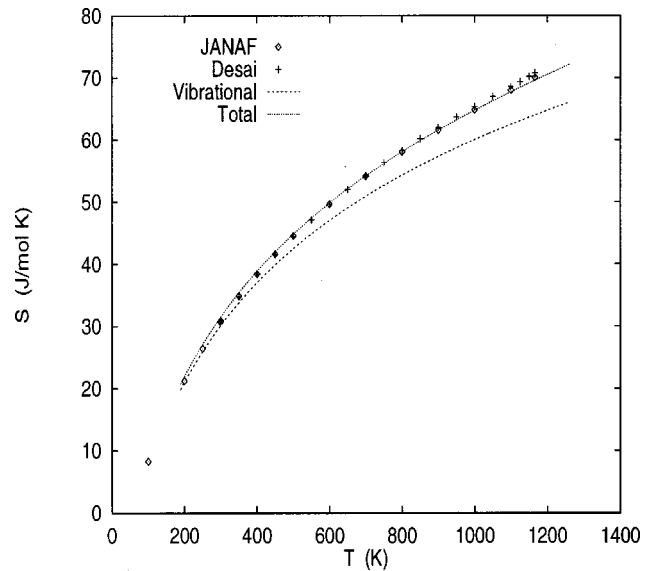
strongly constrain ϕ_0, which is the dominant contribution to the Hugoniot. The volume of metastable ω phase at ambient pressure has been measured[1,3] and has been used in adjusting the parameters. As a crosscheck of our interpretation of the data, we compare our empirically derived ϕ_0 with first principles total energy calculations. This comparison is shown in Fig. 3. For this plot, the band structure energies have been shifted in accordance with our convention that the zero of energy is the minimum of the α phase ϕ_0. There is generally good global agreement between the empirical and first principles curves. For a quantitative comparison, we performed least-squares fits to the band structure energies with the functional form of ϕ_0 given be Eq. (2). The resulting parameters
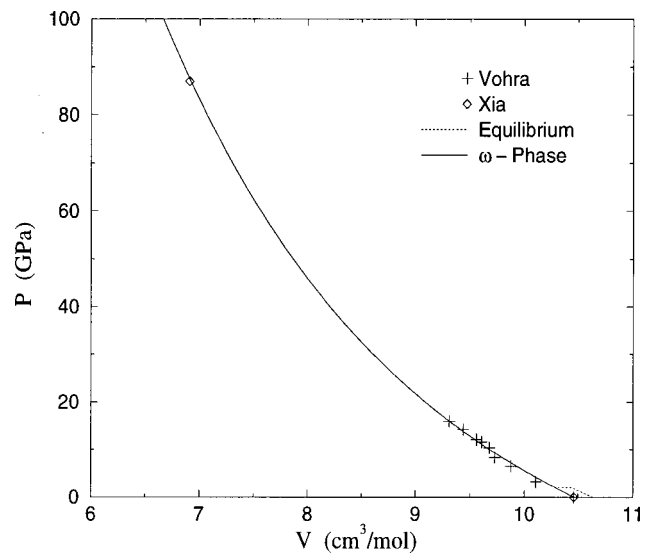
FIG. 2. Room temperature isotherm of Ti. The symbols are experimental data: Refs. 6 and 7. Curves are the present free energy functions. Solid curve is ω phase alone. Dashed curve is two-phase equilibrium. Volume of the ω phase at ambient pressure from Refs. 1 and 3.
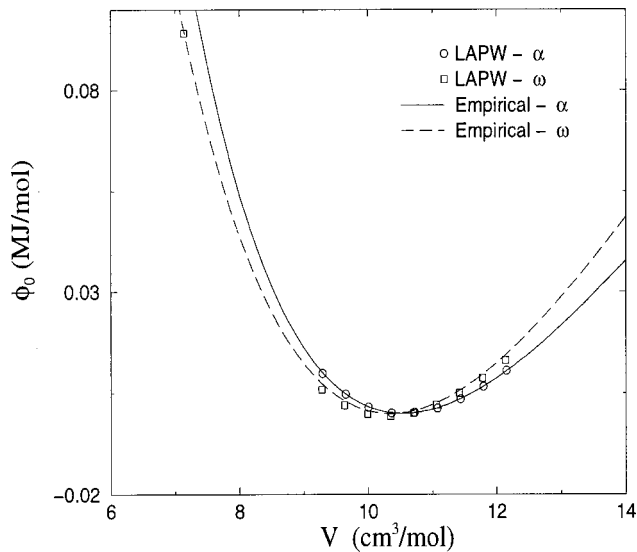
FIG. 3. Static lattice potential $\phi_0(V)$ for α and ω Ti. Symbols are first-principles LAPW calculations. Curves are empirically derived.

FIG. 4. Ti Hugoniot in $U_s - U_p$ plane. Circles are data from Ref. 8, squares from Ref. 11. The solid curve is the equilibrium two-phase Hugoniot. The dashed curve is the metastable α-phase Hugoniot. Dotted curve is for α phase with estimated strength effects based on an HEL of 1.85 GPa.

values for the α phase are $V^* = 10.55\,\text{cm}^3/\text{mol}$, $B^* = 109.6\,\text{GPa}$, $B_1^* = 3.82$. and for the ω-phase $V^* = 10.31\,\text{cm}^3/\text{mol}$, $B^* = 111.5\,\text{GPa}$, $B_1^* = 3.76$. The agreement with the empirical parameters is at the fraction of a percent level for V^*, and $\leqslant 6\%$ for B^*. The level of agreement of B_1^* is not as high, but this is not unexpected for a high-order derivative. The band structure calculations place the minimum energy of the ω phase below that of the α phase. This has been seen in previous band structure calculations.[13,32] The present LAPW energies give $\phi_{0\omega}^* - \phi_{0\alpha}^* = -7.0\,\text{meV/atom}$, whereas the empirical free energy gives $\phi_{0\omega}^* - \phi_{0\alpha}^* = -0.6\,\text{meV/atom}$. Thus, it appears that the electronic structure calculations give too low an energy of the ω phase with respect to α by $\sim 6.4\,\text{meV/atom}$. This is a rather small energy, and is possibly near the limits of accuracy of the electronic structure method. There is also some uncertainty in the empirical energies, which is primarily related to the uncertainty in the location of the equilibrium phase boundary. We expect that there may be errors on the order of 2 meV in the free energy parameter ϕ_0^* on this basis.

Figure 4 shows the Hugoniot data of McQueen et al.[8] along with the recently published data from Trunin et al.[11] in the $U_s - U_p$ (shock velocity–particle velocity) plane. Also shown are our calculations for the equilibrium two-phase Hugoniot, and the metastable α-phase Hugoniot. The curved labeled "α with strength" is for the metastable α phase with strength effects estimated using a Hugoniot elastic limit of 1.85 GPa.[8] We see that the data are consistent with each other. Our interpretation is that the low pressure Hugoniot data correspond to metastable α phase. The data then crossover and join onto the ω phase at high pressure. The flat region in the crossover is presumed to correspond to the existence of a two-wave structure, during which the measured wave speed corresponds to the faster of the waves. The two-wave region shows substantial scatter, being roughly in the range $5.5 < U_s < 5.65$. Figure 5 shows the Hugoniot in the
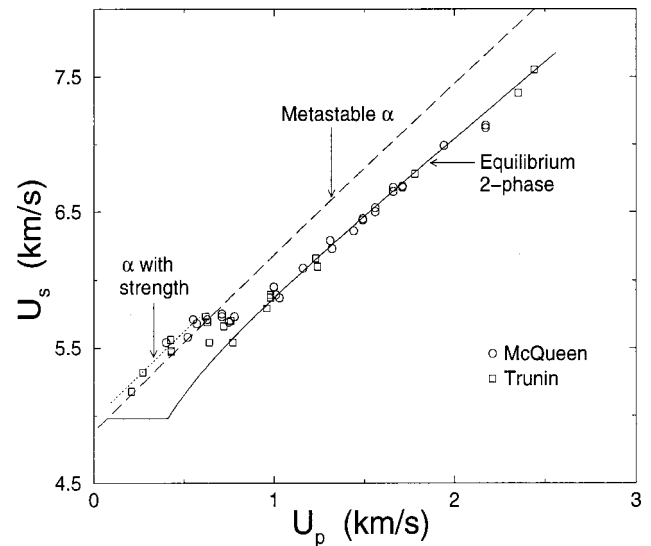
pressure-volume plane. The onset of the transition region is much less distinct in these variables, so the ranges for the start and end of the two-wave region corresponding to the shock velocities in the crossover of Fig. 4 are marked. The phase transition starts at normal stresses in the range $\sim 10.7-14.3$ GPa. This range of transition stresses is consistent with observations of the transition in wave profiles, which give 11.9 GPa (Ref. 9) and 10.4 GPa.[10]

The Hugoniot data of McQueen et al.[8] showed an anomaly, which they identified as a phase transition at 17.5 GPa. Two factors contributed to this interpretation. First, their data set did not extend to sufficiently low pressure to clearly identify the α-phase region. Second they used a value of 5.22 km/s as the bulk sound speed, where the correct
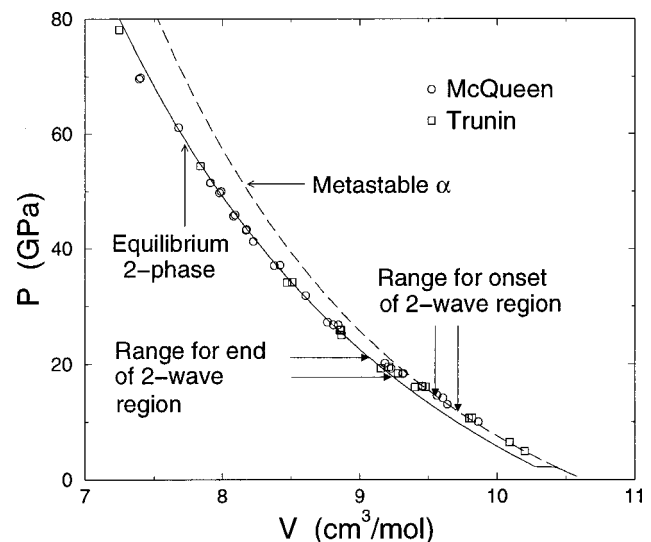
FIG. 5. Ti Hugoniot in pressure-volume plane. The symbols are the same as in Fig. 4. The arrows mark the approximate ranges for the beginning and end of the two-wave region as inferred from the crossover in in Fig. 4.

value is 4.88 km/s. These two factors caused the Hugoniot to appear as two straight segments whose intersection was identified as the transition point. The McQueen *et al.* data are entirely consistent (apart from the bulk sound speed) with the more recent data from Trunin *et al.*,[11] which extend to lower pressure. The lower pressure Hugoniot data, combined with ambient and static high pressure measurements yield a consistent picture. The Hugoniot consists of three segments, an α-phase region, a transition region, and an ω-phase region, with no phase transition at 17.5 GPa.

The present interpretation of the Hugoniot data is well founded on independent data and theory. For instance, our calculated α-phase Hugoniot is constrained by the ambient and static high-pressure data. We have discussed the uncertainty in the parameter B_1^*, which is the most important EOS uncertainty for the Hugoniot. The parameter value we have chosen is at the lower end of the range, consistent with the measured $(\partial B_S / \partial P)_T$. If we take the larger value, consistent with $(\partial B_S / \partial T)_P$, the effect on the Hugoniot is similar to the effect of strength as shown in Fig. 4. While noticeable, this uncertainty is not nearly large enough to change our qualitative picture. Similarly, the ω-phase Hugoniot is well constrained by the static high-pressure data, and the agreement with electronic structure calculations is good.

Boettger and Wallace[15] carried out an extensive analysis of the $\alpha - \epsilon$ transition in shocked Fe. By comparing with a large number of VISAR profiles, they were able to obtain a rather detailed picture of the transition kinetics. In Fe, there are metastable states that are long-lived on the time scale of both shock wave and static measurements. The kinetics in the shock consists of relaxation toward the long-lived metastable state. This relaxation is sufficiently rapid that the observed Hugoniot corresponds to the metastable state, which is essentially the same state obtained in static measurements. The case of Ti provides an interesting contrast. The Ti Hugoniot points extend farther up the metastable α-phase branch than is observed in static measurements, indicating that there is a relaxation process occurring on a time scale intermediate between those of the static and shock measurements.

The kinetics of the $\alpha - \omega$ transformation in shocked Ti are clearly important for understanding the extent of the metastable branch of the Hugoniot, and may play a role in the scatter of the Hugoniot data in the transition region. Data on the kinetics are, however, sparse, and we can make only some general observations. Singh *et al.*[33] have made quantitative observations of the transition kinetics under static pressure. They find a continuously varying relaxation time that depends exponentially on pressure in the range from 5 to 9 GPa. This is qualitatively consistent with the higher transition threshold in shock waves, given that the time allowed for the transition is orders of magnitude shorter than in the static case. However, extrapolation from the static measurements gives a pressure of 19 GPa to reach a rate of 1 μs^{-1}. Evidently the transformation occurs more rapidly in the shock than indicated by extrapolating the static data.

The fact that the apparent shock transition threshold is $\sim$10 GPa above the equilibrium phase boundary is somewhat unusual. This may be attributed to the small volume change, which leads to a small driving force ΔG at a given pressure. At 12 GPa on the Hugoniot, $\Delta G = 1.2 \times 10^3$ J/mol. This is not unusually large,[34] and is comparable to the estimated strain energy barrier for the transition.[34]

A measurement of the stress history $\sigma(t)$ showing the transition in a shock experiment was published by Kutsar.[9] Rather than showing a distinct third wave corresponding to the phase transition, Kutsar's profile consists of a ramp-like wave connecting the start of the transition to the final state. This type of profile shows a strong kinetic influence, and is typical of the case where the first plastic wave is decaying with propagation distance into the sample.[28] Kutsar's measurements were taken 15 mm into the sample, suggesting that measurements on thinner samples may show a dependence of the apparent transition stress on sample thickness.

Vohra *et al.*[5] made observations of samples with differing purity under static high pressure, and found the transformation occurred more slowly at a given P in a sample with 3800 ppm oxygen than in one with 927 ppm oxygen. Gray *et al.*[10] observed a three-wave structure associated with the transition in velocity interferometry (VISAR) measurements on a shocked sample of high-purity Ti. They also found retained ω phase in recovered high-purity samples shocked to 11 GPa. Neither of these indications of the transition were observed in a sample with 3700 ppm oxygen. These results show a significant impact from small amounts of oxygen. Unfortunately, most of the shock data refer to samples of unspecified purity. There appears to be a significant dependence of the kinetic parameters of the transition on oxygen concentration. A logical next step in mapping this phenomenon would be to work out the dependence of the transition rate on oxygen concentration. This would require taking VISAR profiles on samples with controlled variations of oxygen concentration.

IV. SUMMARY AND CONCLUSIONS

In summary, we have presented parametrized equilibrium free energies for α and ω Ti. These thermodynamic functions reconcile the existing ambient, static high-pressure, and shock data, and are consistent with first principles total energy calculations. The interpretation of the Hugoniot data seems clear. The Hugoniot states lie on the metastable α-phase branch to pressures $\sim$12 GPa where the transformation to the β-phase begins. The extent of the metastability is larger than is seen in static experiments, in contrast to the well-studied case of Fe.[15] There is generally a pronounced influence of kinetics on the shock-wave observations of the transition, but this has not been systematically investigated to the extent that would allow a phenomenological description of the transition rate. It would be interesting to develop such a description, and to work out the dependence of the parameters on the oxygen concentration.

[1] J. C. Jamieson, Science **140**, 72 (1963).

[2] F. P. Bundy, General Electric Research Laboratory Report No. 63-RL-3481 C (1963).

[3] V. A. Zilbershteyn, G. I. Nosova, and E. I. Estrin, Fiz. Met. Metalloved. **35**, 584 (1973).

[4] V. A. Zilbershteyn, N. P. Chistotina, A. A. Zharov, N. S. Grishina, and E. I. Estrin, Fiz. Met. Metalloved. **39**, 445 (1975).

[5] Y. K. Vohra, S. K. Sikka, S. N. Vaidya, and R. Chidambaram, J. Phys. Chem. Solids **38**, 1293 (1977).

[6] Y. K. Vohra, H. Olijnyk, W. Grosshans, and W. B. Holtzapfel, in *High Pressure in Research and Industry*, edited by C. M. Backman, T. Johannisson, and L. Tegner (Arkitektkopia, Uppsala, Sweden 1982).

[7] H. Xia, G. Parthasarathy, H. Luo, Y. K. Vohra, and A. L. Ruoff, Phys. Rev. B **42**, 6736 (1990).

[8] R. G. McQueen, S. P. Marsh, J. W. Taylor, J. N. Fritz, and W. J. Carter, in *High Velocity Impact Phenomena*, edited by R. Kinslow (Academic, New York, 1970).

[9] A. R. Kutsar, M. N. Pavlovskii, and V. V. Komissarov, JETP Lett. **35**, 108 (1982).

[10] G. T. Gray, C. E. Morris, and A. C. Lawson, in *Titanium '92 Science and Technology*, edited by F. H. Froes and I. Caplan (Minerals, Metals, and Materials Society, 1993).

[11] R. F. Trunin, G. V. Simakov, and A. B. Medvedev, High Temp. **37**, 851 (1999).

[12] O. Eriksson, J. M. Wills, and D. Wallace, Phys. Rev. B **46**, 5221 (1992).

[13] R. Ahuja, J. M. Wills, B. Johansson, and O. Eriksson, Phys. Rev. B **48**, 16269 (1993).

[14] D. B. Hayes, J. Appl. Phys. **45**, 1208 (1974).

[15] J. C. Boettger and D. C. Wallace, Phys. Rev. B **55**, 2840 (1997).

[16] J. H. Rose, J. R. Smith, F. Guinea, and J. Ferrante, Phys. Rev. B **29**, 2963 (1984).

[17] D. C. Wallace, *Thermodynamics of Crystals* (Dover, Mineola, 1998).

[18] L. D. Landau and E. M. Lifshitz, *Statistical Physics, Part 1* (Pergamon, Oxford, 1980), Sec. 65.

[19] O. L. Anderson, *Equations of State of Solids for Geophysics and Ceramic Science* (Oxford University Press, Oxford, 1995).

[20] D. C. Wallace, Proc. R. Soc. London, Ser. A **433**, 631 (1991).

[21] M. W. Chase, Jr., C. A. Davies, J. R. Downey, Jr., D. J. Frurip, R. A. McDonald, and A. N. Syverud, J. Phys. Chem. Ref. Data Suppl. **14**, 1 (1985).

[22] P. D. Desai, Int. J. Thermophys. **8**, 781 (1987).

[23] G. Simmons and H. Wang, *Single Crystal Elastic Constants and Calculated Aggregate Properties: A Handbook* (MIT Press, Cambridge, MA, 1971).

[24] E. S. Fisher and M. H. Manghnani, J. Phys. Chem. Solids **32**, 657 (1971).

[25] Y. S. Touloukian, R. K. Kirby, R. E. Taylor, and P. D. Desai, *Thermal Expansion: Metallic Elements and Alloys* (IFI/Plenum, New York, 1975).

[26] W. Petry, A. Heiming, J. Trampenau, M. Alba, C. Herzig, H. R. Schober, and G. Vogl, Phys. Rev. B **43**, 10933 (1991).

[27] W. B. Pearson, *A Handbook of Lattice Spacings and Structures of Metals and Alloys* (Pergamon, New York, 1958).

[28] G. E. Duval and R. A. Graham, Rev. Mod. Phys. **49**, 523 (1977).

[29] P. Blaha, K. Schwarz, and J. Luitz, WIEN97, Vienna University of Technology, 1997. [Improved and updated Unix version of the original copyrighted WIEN-code, which was published by P. Blaha, K. Schwarz, P. Sorantin, and S. B. Trickey, Comput. Phys. Commun. **59**, 399 (1990)].

[30] J. P. Perdew, S. Burke, and M. Ernzerhof, Phys. Rev. Lett. **77**, 3865 (1996).

[31] P. E. Bloechl, O. Jepsen, and O. K. Anderson, Phys. Rev. B **49**, 16223 (1994).

[32] G. Jomard, L. Magaud, and A. Pasturel, Philos. Mag. B **77**, 67 (1998).

[33] A. K. Singh, M. Mohan, and C. Divkar, J. Appl. Phys. **53**, 1221 (1982).

[34] E. I. Estrin, Fiz. Met. Metalloved. **37**, 1249 (1974).